Appendix A: Additional mesh information

As was described in section 6.3 the geometry of labyrinth seal was divided into specific areas (see Figure 6-1) based on the shape and fluid flow through labyrinth seal. Than grid was applied on each area, that was divided into finer cells near the wall or boundary edges (regions) using geometrical series starting from the middle of the edge of each section. Number of horizontal or vertical divisions was calculated from eq. 6-35 and noted in Table 8-1, based on dimensions of chosen area and initial cell distance a_0 using growth rate equals to 1,2 .

Example of grid evaluation is shown for Area **A** with the lowest resolution (a_0=0,1 mm). The edges of area A are than 1,5 and 4,5 mm (see Figure 6-1). From Table 8-1 is obvious that horizontal number of cell division is 10 and vertical is 19. The grid of Area A is shown at Figure 8-1.

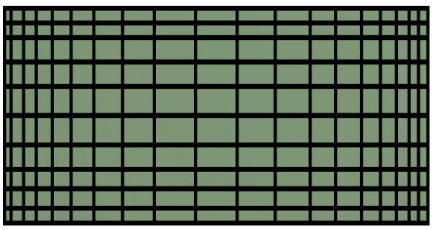

Figure 9-1 Area A, lowest grid resolution

Table 9-1 Number of cell division

Number of vertical and horizontal cell divisions of grid section based on eq.6-35 [-]

Mesh type		1	2	3	4	5	6	7	8
a_0 [mm]		0,1	0,05	0,01	0,005	0,001	0,0005	0,0001	0,0001
q [-]		1,2	1,2	1,2	1,2	1,2	1,2	1,2	1,1
D [mm]	0,30	3	5	15	21	38	45	63	105
	0,50	4	8	20	26	43	51	68	116
	1,50	10	15	30	38	55	63	80	139
	1,90	12	17	33	40	58	65	83	144
	2,00	12	18	33	41	58	66	83	145
	2,08	12	18	34	41	59	66	84	146
	3,15	16	22	38	46	63	71	88	154
	3,25	16	22	39	46	63	71	89	155
	3,85	17	24	40	48	65	73	91	159
	3,95	18	24	41	48	66	73	91	159
	4,00	18	24	41	48	66	73	91	160
	4,50	19	25	42	49	67	75	92	162

Appendix B: Static pressure of each turbulent model

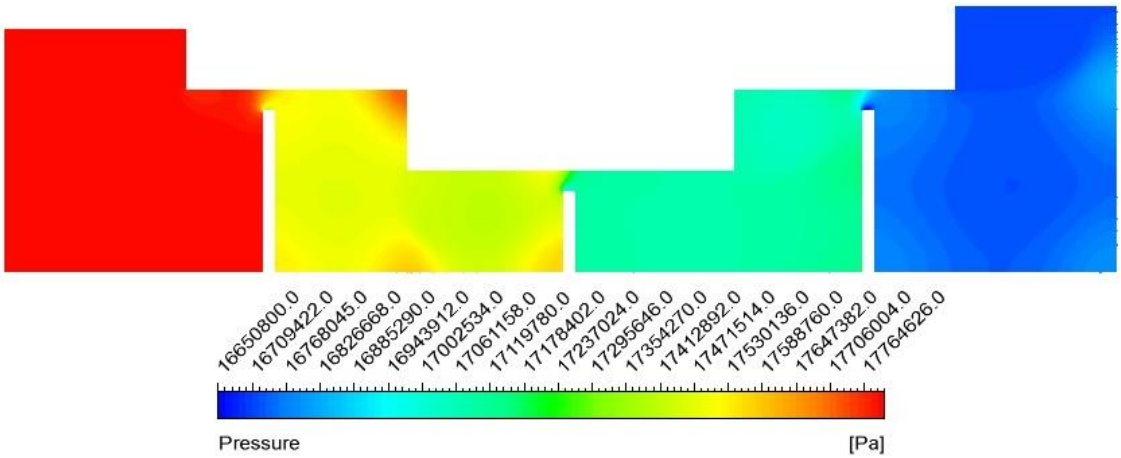

Figure 9-2 Static pressure of fluid using k-ε model

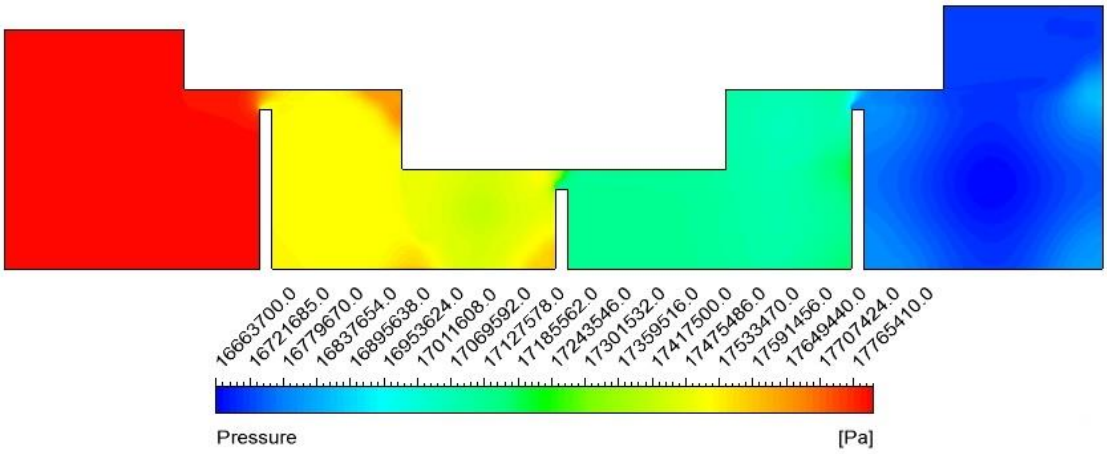

Figure 9-3 Static pressure of fluid using Reynolds stress model

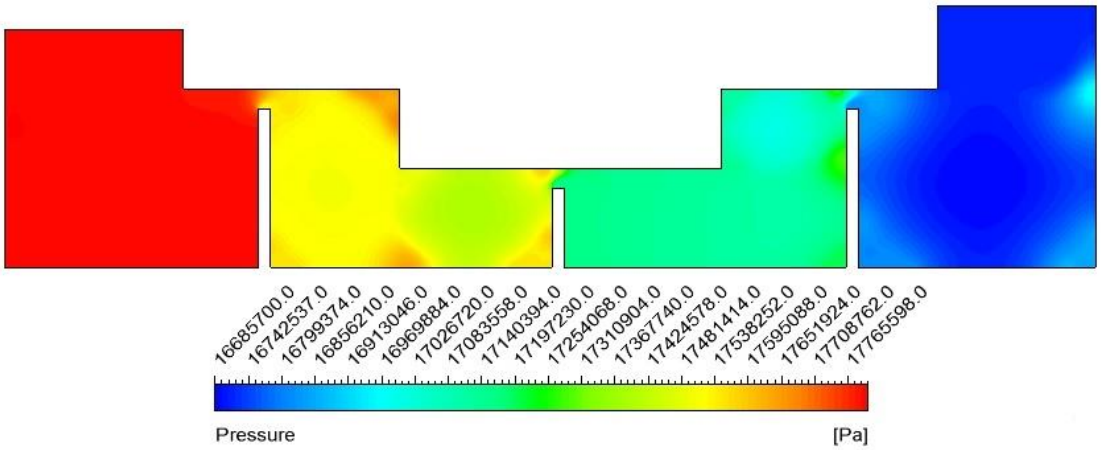

Figure 9-4 Static pressure of fluid using SST k-ω model

Table 9-2 Mass flow rate results for high pressure boundary conditions

MASS FLOW RATES RESULTS OF EXISTING LEAKAGE MODELS AND CFD SIMULATIONS FOR HIGH PRESSURE BOUNDARY CONDITIONS [kg/s]

MODEL	Pressure ratio [-]															
	0,94	0,90	0,85	0,80	0,75	0,70	0,65	0,60	0,55	0,50	0,45	0,40	0,35	0,30	0,25	0,20
STANDARD k-ε	**2,0279**	**2,5565**	**3,0766**	**3,4969**	**3,8500**	**4,1539**	**4,4183**	**4,6502**	**4,8542**	**5,0322**	**5,1866**	**5,3190**	**5,4287**	**5,5177**	**5,5839**	**5,6261**
SAMOYLOVICH	2,4696	3,1154	3,7464	4,2405	4,6435	4,9776	5,2559	5,4870	5,6765	5,8286	5,9462	6,0312	6,0850	6,1084	6,1019	6,0652
STODOLA	2,5103	3,1806	3,8472	4,3819	4,8306	5,2155	5,5499	5,8425	6,0993	6,3247	6,5219	6,6934	6,8412	6,9667	7,0712	7,1556
AUNGIER	2,6352	3,2423	3,8558	4,3555	4,7797	5,1461	5,4651	5,7438	5,9870	6,1985	6,3814	6,5382	6,6708	6,7812	6,8710	6,9417
KEARTON	2,4842	3,1252	3,7444	4,2220	4,6047	4,9151	5,1668	5,3686	5,5264	5,6447	5,7268	5,7751	5,7919	5,7792	5,7388	5,6729
ZALF	3,5023	4,4069	5,2822	5,9595	6,5049	6,9507	7,3161	7,6135	7,8515	8,0358	8,1707	8,2585	8,3005	8,2964	8,2440	8,1379

Table 9-3 Percentage deviation between numerical and analytical data for high pressure boundary conditions

PERCENTAGE DEVIATION BETWEEN EXISTING LEAKAGE MODELS AND CFD SIMULATION RESULTS FOR HIGH PRESSURE BOUNDARY CONDITIONS [%]

MODEL	Pressure ratio [-]																AVERAGE
	0,94	0,90	0,85	0,80	0,75	0,70	0,65	0,60	0,55	0,50	0,45	0,40	0,35	0,30	0,25	0,20	[%]
SAMOYLOVICH	-21,8	-21,9	-21,8	-21,3	-20,6	-19,8	-19,0	-18,0	-16,9	-15,8	-14,6	-13,4	-12,1	-10,7	-9,3	-7,8	-16,5
STODOLA	-23,8	-24,4	-25,0	-25,3	-25,5	-25,6	-25,6	-25,6	-25,7	-25,7	-25,7	-25,8	-26,0	-26,3	-26,6	-27,2	-25,6
AUNGIER	-30,0	-26,8	-25,3	-24,6	-24,1	-23,9	-23,7	-23,5	-23,3	-23,2	-23,0	-22,9	-22,9	-22,9	-23,1	-23,4	-24,2
KEARTON	-22,5	-22,2	-21,7	-20,7	-19,6	-18,3	-16,9	-15,4	-13,8	-12,2	-10,4	-8,6	-6,7	-4,7	-2,8	-0,8	-13,6
ZALF	-72,7	-72,4	-71,7	-70,4	-69,0	-67,3	-65,6	-63,7	-61,7	-59,7	-57,5	-55,3	-52,9	-50,4	-47,6	-44,6	-61,4

Table 9-4 Mass flow rate results for intermedial pressure boundary conditions

MASS FLOW RATES RESULTS OF EXISTING LEAKAGE MODELS AND CFD SIMULATIONS FOR INTERMEDIAL PRESSURE BOUNDARY CONDITIONS [kg/s]

MODEL	Pressure ratio [-]														
	0,90	0,85	0,80	0,75	0,70	0,65	0,60	0,55	0,50	0,45	0,40	0,35	0,30	0,25	0,20
STANDARD k-ε	**0,5012**	**0,6030**	**0,6852**	**0,7543**	**0,8138**	**0,8657**	**0,9113**	**0,9514**	**0,9864**	**1,0168**	**1,0433**	**1,0657**	**1,0840**	**1,0981**	**1,1074**
SAMOYLOVICH	0,5683	0,6828	0,7729	0,8463	0,9072	0,9580	1,0001	1,0346	1,0623	1,0838	1,0993	1,1091	1,1133	1,1121	1,1055
STODOLA	0,5802	0,7012	0,7987	0,8804	0,9506	1,0115	1,0649	1,1117	1,1528	1,1887	1,2200	1,2469	1,2698	1,2888	1,3042
AUNGIER	0,5915	0,7028	0,7939	0,8712	0,9379	0,9961	1,0469	1,0912	1,1298	1,1631	1,1917	1,2158	1,2360	1,2523	1,2652
KEARTON	0,5701	0,6825	0,7695	0,8393	0,8958	0,9417	0,9785	1,0073	1,0288	1,0438	1,0526	1,0557	1,0533	1,0460	1,0340
ZALF	0,8039	0,9627	1,0862	1,1856	1,2669	1,3335	1,3877	1,4310	1,4646	1,4892	1,5052	1,5129	1,5121	1,5026	1,4832

Table 9-5 Percentage deviation between numerical and analytical data for intermedial pressure boundary conditions

PERCENTAGE DEVIATION BETWEEN EXISTING LEAKAGE MODELS AND CFD SIMULATION RESULTS FOR INTERMEDIAL PRESSURE BOUNDARY CONDITIONS [%]

MODEL	Pressure ratio [-]															AVERAGE
	0,90	0,85	0,80	0,75	0,70	0,65	0,60	0,55	0,50	0,45	0,40	0,35	0,30	0,25	0,20	[%]
SAMOYLOVICH	-13,4	-13,2	-12,8	-12,2	-11,5	-10,7	-9,7	-8,8	-7,7	-6,6	-5,4	-4,1	-2,7	-1,3	0,2	-8,0
STODOLA	-15,8	-16,3	-16,6	-16,7	-16,8	-16,8	-16,8	-16,9	-16,9	-16,9	-16,9	-17,0	-17,1	-17,4	-17,8	-16,8
AUNGIER	-18,0	-16,5	-15,9	-15,5	-15,2	-15,1	-14,9	-14,7	-14,5	-14,4	-14,2	-14,1	-14,0	-14,0	-14,2	-15,0
KEARTON	-13,8	-13,2	-12,3	-11,3	-10,1	-8,8	-7,4	-5,9	-4,3	-2,7	-0,9	0,9	2,8	4,7	6,6	**-5,0**
ZALF	-60,4	-59,7	-58,5	-57,2	-55,7	-54,0	-52,3	-50,4	-48,5	-46,5	-44,3	-42,0	-39,5	-36,8	-33,9	-49,3

Table 9-6 Mass flow rate results for low pressure boundary conditions

MASS FLOW RATES RESULTS OF EXISTING LEAKAGE MODELS AND CFD SIMULATIONS FOR LOW PRESSURE BOUNDARY CONDITIONS [kg/s]

MODEL	Pressure ratio [-]														
	0,90	0,85	**0,80**	0,75	0,70	0,65	0,60	0,55	0,50	0,45	0,40	0,35	0,30	0,25	0,20
STANDARD k-ε	**0,0740**	**0,0895**	**0,1022**	**0,1130**	**0,1224**	**0,1306**	**0,1380**	**0,1446**	**0,1505**	**0,1558**	**0,1606**	**0,1649**	**0,1687**	**0,1721**	**0,1750**
SAMOYLOVICH	0,0722	0,0866	0,0980	0,1072	0,1148	0,1211	0,1263	0,1305	0,1339	0,1365	0,1383	0,1394	0,1398	0,1395	0,1386
STODOLA	0,0737	0,0890	0,1012	0,1115	0,1203	0,1279	0,1345	0,1403	0,1453	0,1497	0,1535	0,1567	0,1595	0,1617	0,1635
AUNGIER	0,0751	0,0892	0,1006	0,1103	0,1187	0,1259	0,1322	0,1377	0,1424	0,1465	0,1499	0,1528	0,1552	0,1571	0,1586
KEARTON	0,0724	0,0866	0,0975	0,1063	0,1133	0,1190	0,1236	0,1271	0,1297	0,1314	0,1324	0,1327	0,1323	0,1312	0,1296
ZALF	0,1021	0,1221	0,1377	0,1501	0,1603	0,1685	0,1752	0,1805	0,1846	0,1875	0,1894	0,1902	0,1899	0,1885	0,1859

Table 9-7 Percentage deviation between numerical and analytical data for low pressure boundary condition

PERCENTAGE DEVIATION BETWEEN EXISTING LEAKAGE MODELS AND CFD SIMULATION RESULTS FOR LOW PRESSURE BOUNDARY CONDITIONS [%]

MODEL	Pressure ratio [-]															AVERAGE
	0,90	0,85	**0,80**	0,75	0,70	0,65	0,60	0,55	0,50	0,45	0,40	0,35	0,30	0,25	0,20	[%]
SAMOYLOVICH	2,4	3,2	4,2	5,1	6,2	7,3	8,5	9,7	11,0	12,4	13,9	15,4	17,1	18,9	20,8	10,4
STODOLA	0,4	0,6	1,0	1,3	1,7	2,1	2,5	3,0	3,4	3,9	4,4	4,9	5,5	6,0	6,6	**3,2**
AUNGIER	-1,5	0,4	1,6	2,4	3,0	3,6	4,2	4,8	5,4	6,0	6,6	7,3	8,0	8,7	9,4	4,6
KEARTON	2,1	3,3	4,6	5,9	7,4	8,9	10,4	12,1	13,8	15,6	17,5	19,5	21,6	23,7	25,9	12,8
ZALF	-38,0	-36,4	-34,7	-32,9	-31,0	-29,0	-27,0	-24,9	-22,7	-20,4	-17,9	-15,3	-12,6	-9,6	-6,3	-23,9

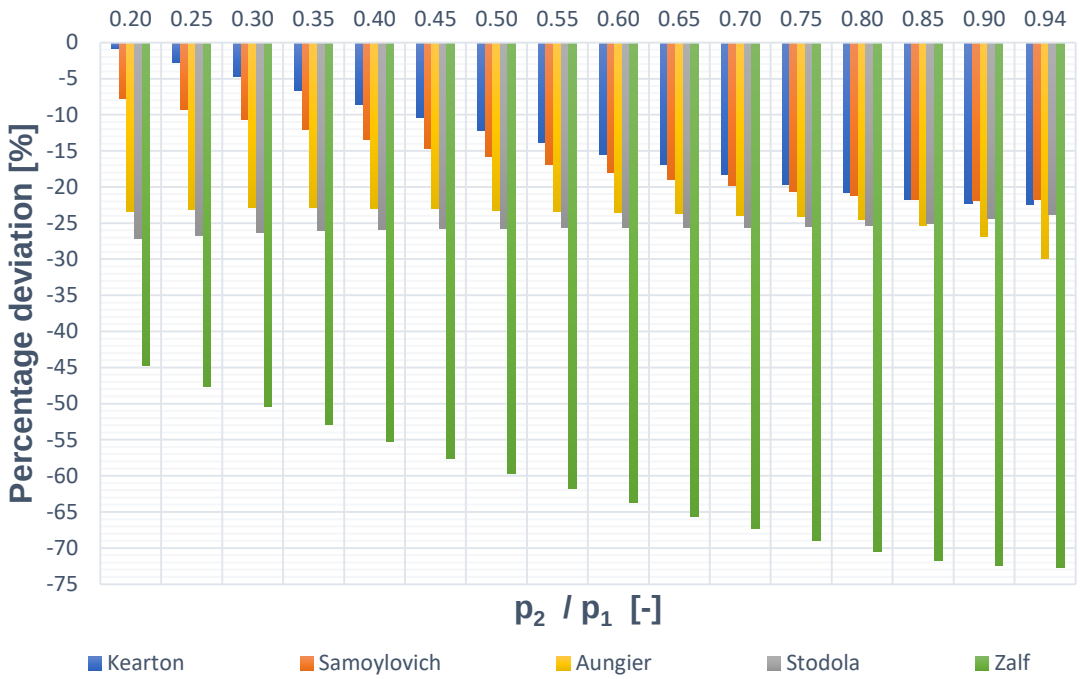

Figure 9-5 Percentage difference between numerical and analytical data for high pressure boundary conditions

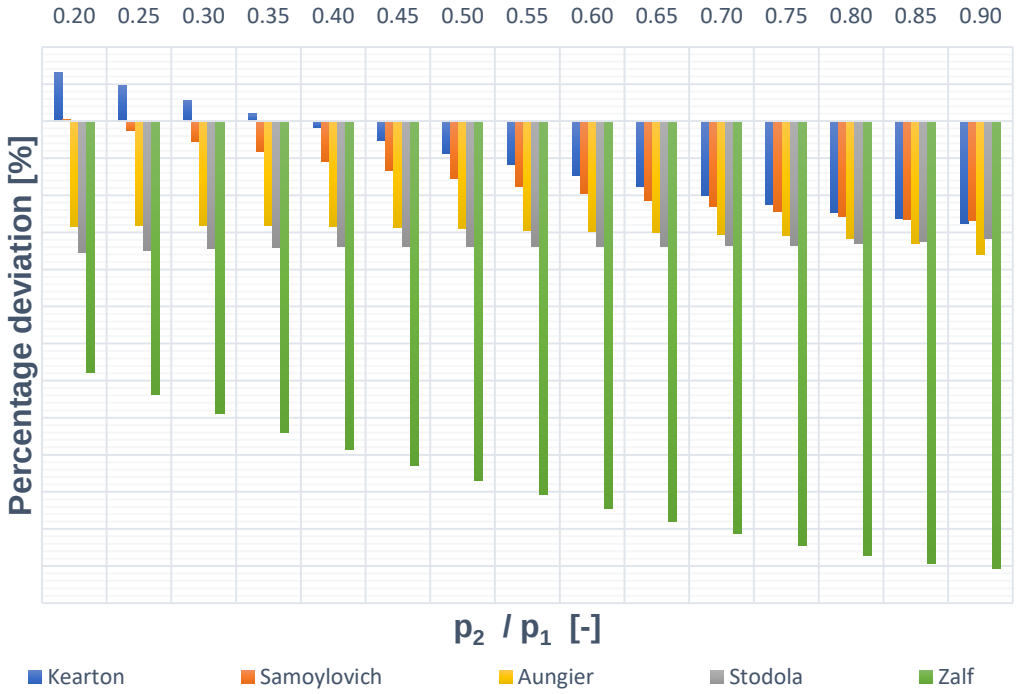

Figure 9-6 Percentage difference between numerical and analytical data for intermedial pressure boundary conditions

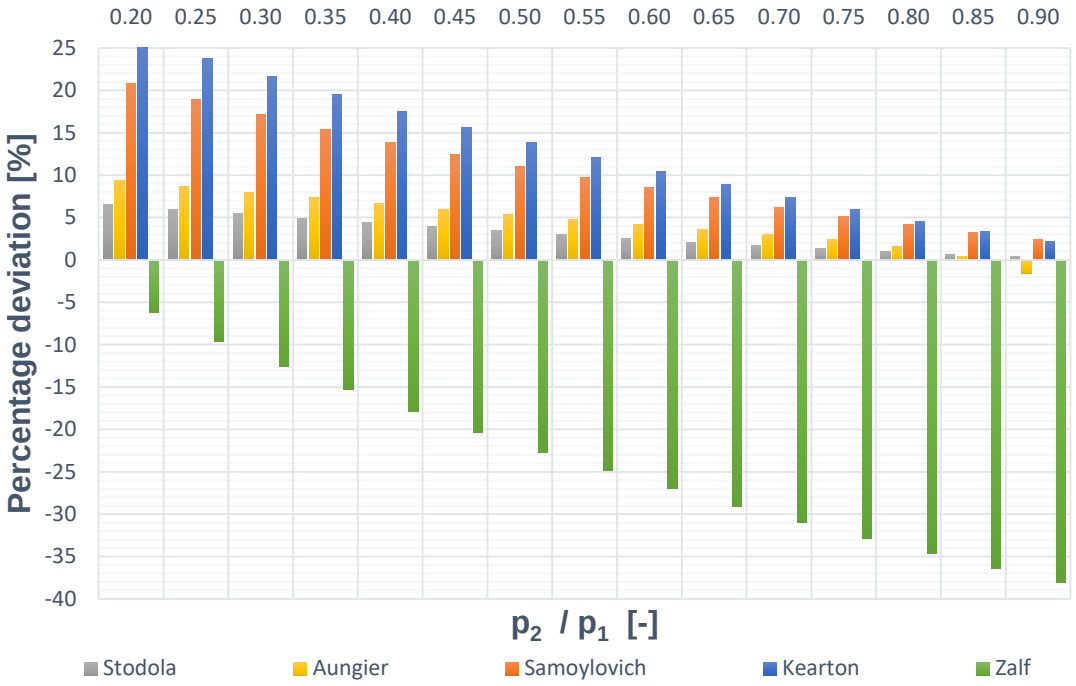

Figure 9-7 Percentage difference between numerical and analytical data for low pressure boundary conditions